OBJECTIVE ASSESSMENT OF RENAL DCE-MRI IMAGE SEGMENTATION

B. Chevaillier[(1)], *J.-L. Collette*[(1)], *D. Mandry*[(2,3)], *M. Claudon*[(2,3)] *and O. Pietquin*[(1,2,3)]

[(1)] IMS Research Group,
Supelec Metz Campus, 57070, Metz, France
phone: + (33) 387 764 711 , fax: + (33) 387 764 700, email: Beatrice.Chevaillier@supelec.fr
web: http://ims.metz.supelec.fr/

[(2)] Inserm, U947
CHU Nancy Brabois, 54500, Vandoeuvre-les-Nancy, France

[(3)] IADI,
Nancy University, 54500, Vandoeuvre-les-Nancy, France

ABSTRACT

In dynamic contrast-enhanced magnetic resonance imaging (DCE-MRI) of renal perfusion with injection of a contrast agent, the segmentation of kidney in regions of interest like cortex, medulla and pelvo-caliceal cavities is necessary for accurate functional evaluation. Several semiautomatic segmentation methods using time-intensity curves of renal voxels have been recently developed. Most of the time, quantitative result validation consists in comparisons with a manual segmentation by an expert. However it can be questionable to consider such a segmentation as a ground truth, especially because of intra- and inter-operator variability. Moreover it makes comparisons between results published by different authors delicate. We propose a method to built synthetic DCE-MRI sequences from typical time-intensity curves and an anatomical model that can be used for objective assessment of renal internal structures.

1. INTRODUCTION

Perfusion dynamic contrast-enhanced magnetic resonance imaging (DCE-MRI) with injection of a contrast agent like gadolinium chelates is widely used for renal assessment. The segmentation of kidney in regions of interest like cortex, medulla and pelvo-caliceal cavities is necessary for accurate functional evaluation. In order to avoid tedious and time-consuming manual segmentation, semiautomatic methods for segmentation of internal renal structures have been recently developed ; most of them are based on the analysis of time-intensity curves of renal pixels [1, 2, 3, 4, 5, 6, 7]. Validation is mostly performed by comparing the resulting segmentations with a manual one. However it can be questionable to consider such a segmentation as a ground truth or a gold standard, even if it is done by an expert. It is indeed subject to intra- and inter-operator variability, especially because of some subjectivity in gray-level based boundary delineation. It is thus difficult to know whether errors are linked with this variability or the tested algorithm is not really efficient and should be improved. Moreover it makes comparisons between results published by different authors delicate. A method for objective segmentation assessment would be worthwhile. We propose to generate synthetic DCE-MRI sequences of renal perfusion with contrast agent injection for normal and pathological kidneys from typical time-intensity curves and an anatomical model. This model can be used as a ground truth for segmentation validation.

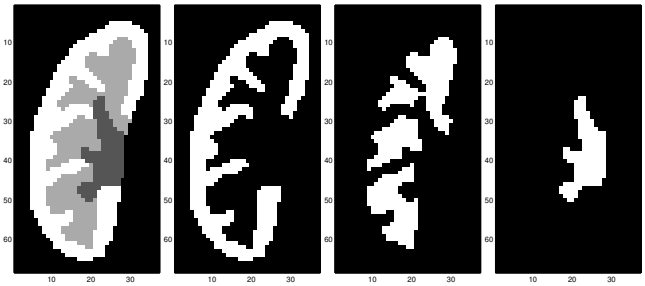

FIG. 1 – Hard segmentation of a kidney in three compartments (a) : cortex, medulla and cavities (respectively light, medium and dark gray) and corresponding binary segmentations (b to d)

2. BASIC MODEL DESCRIPTION

2.1 Main ideas

We confine ourselves to a 2D model in order to generate only one slice, but a 3D one could be built in the same way. The main elements of our model are a 2 dimensional anatomical representation of a kidney slice with three compartments and four average perfusion curves (one for each renal compartment and one for neighboring organs). Our purpose is not to simulate the whole MRI acquisition process with slice reconstruction but to get simply a series of sufficiently realistic frames to test segmentation algorithms.

2.1.1 Anatomical model

The kidney is represented by a matrix corresponding to its segmentation in three anatomical compartments with a given spatial resolution. Because renal structures are usually thinner than a voxel, each of them is a mixture of several compartments and of other organs. Each element j of the matrix is thus a quadruplet $\{\alpha_j^{(i)}\}, 1 \leq i \leq 4$ giving the proportion of cortex, medulla, cavities and other organs for

 ISSN 2076-1465

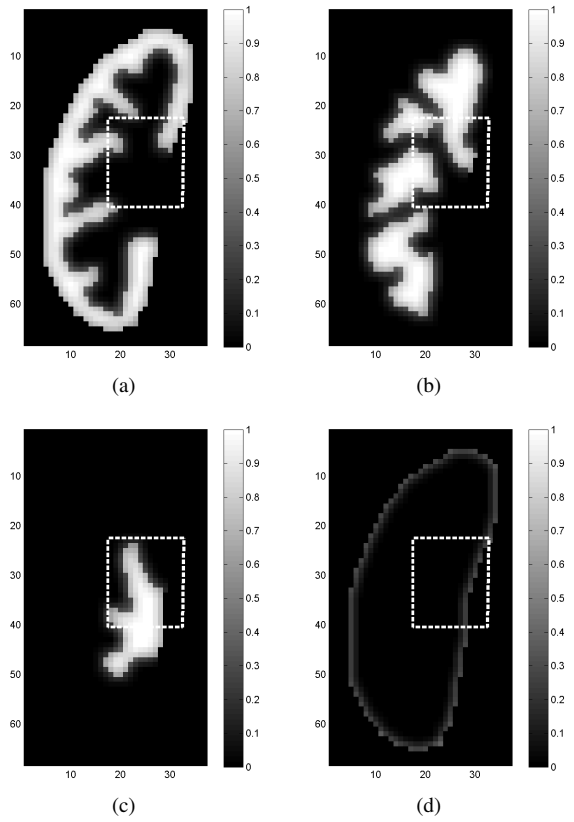

FIG. 2 – Example of a anatomical renal model with three internal compartments with the proportions of cortex (a), medulla (b), cavities (c) and other organs (d) for each voxel.

voxel j. Plausible proportions can be obtained simply from a hard segmentation (figure 1) by filtering every corresponding binary segmentation with a same two-dimensional low-pass FIR filter F

$$F = \begin{pmatrix} c_2 & c_2 & c_2 & c_2 & c_2 \\ c_2 & c_1 & c_1 & c_1 & c_2 \\ c_2 & c_1 & c_0 & c_1 & c_2 \\ c_2 & c_1 & c_1 & c_1 & c_2 \\ c_2 & c_2 & c_2 & c_2 & c_2 \end{pmatrix} \text{ with } \sum_{i,j} F_{ij} = 1 \qquad (1)$$

For the example in figure 2, with details in figure 3, $c_0 = 0.4, c_1 = 0.045$ and $c_2 = 0.015$. The composition of any voxel of the hard segmentation is thus modulated by including a percentage of its 24-nearest neighbors : this takes into account that voxels located on the boundaries between different compartments are a mixture of them. The relative values of filter coefficients can be adjusted to increase or reduce the mixture.

2.1.2 Time-intensity curves of renal voxels

For each compartment a time-intensity curve is then defined : it constitute a typical contrast evolution of a voxel that would contain only one type of tissue, without acquisition noise (see example in figure 4). Even if exterior organs can have fairly different contrast evolution, they are represented by a single average curve for the sake of simplicity. In the proposed example these curves $I_i(t), 1 \leq i \leq 4$ are obtained by denoising average curves from real data.

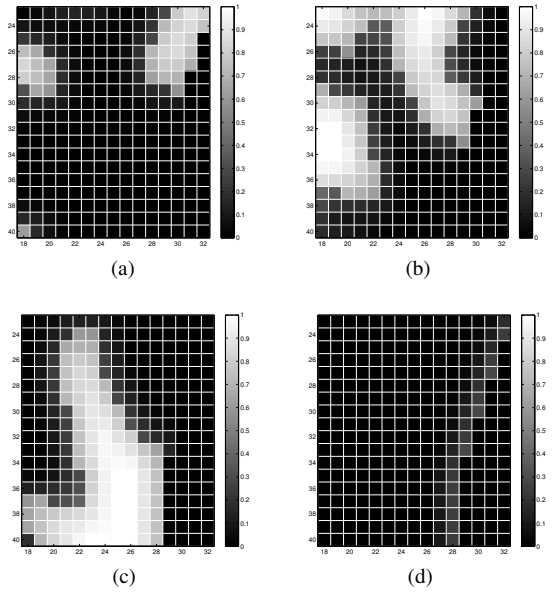

FIG. 3 – Example of a anatomical renal model with three internal compartments with the proportions of cortex (a), medulla (b), cavities (c) and other organs (d) for each voxel : zoom on selected area in figure 3

3. MODELLED PHENOMENA

To build realistic sequences using the above anatomical model and the curves $I_i(t), 1 \leq i \leq 4$, different phenomena are taken into account according to the flow chart in figure 5.

3.1 Partial volume effect

Signal intensity $I(j,t)$ for a given voxel j at time t is a linear combination of the contributions of the different tissues it contains [8] : this is known as the Partial Volume Effect (PVE). For a model with C compartments, let $\alpha_j^{(i)}$ be the proportion of tissue i in voxel j :

$$I(j,t) = \sum_{i=1}^{C} \alpha_j^{(i)} I_i(t) \text{ with } \sum_{i=1}^{C} \alpha_j^{(i)} = 1 \text{ et } 0 \leq \alpha_j^{(i)} \leq 1 \qquad (2)$$

A first series of frames can thus be built thanks to the anatomical model and the curves $I_i(t), 1 \leq i \leq 4$ (figure 6a and b).

3.1.1 Dominant anatomical compartment

The dominant anatomical compartment for voxel j is compartment k with :

$$k = \arg\max_i \alpha_j^{(i)} \qquad (3)$$

and should be recovered with any consistent segmentation method.

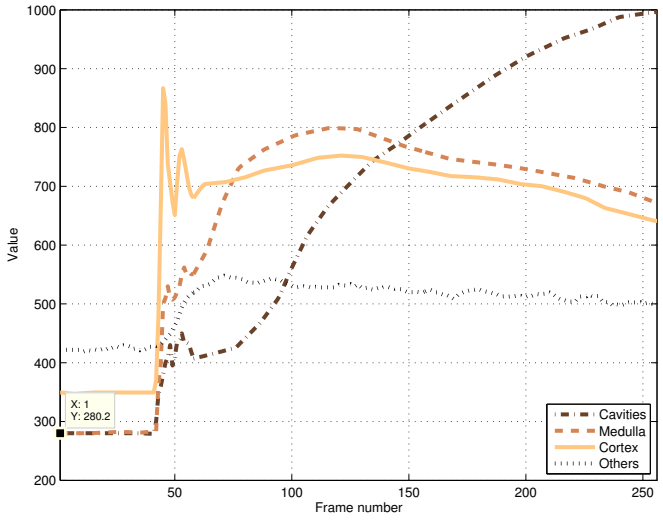

FIG. 4 – Typical time-intensity curves for the three renal compartments and for other organs

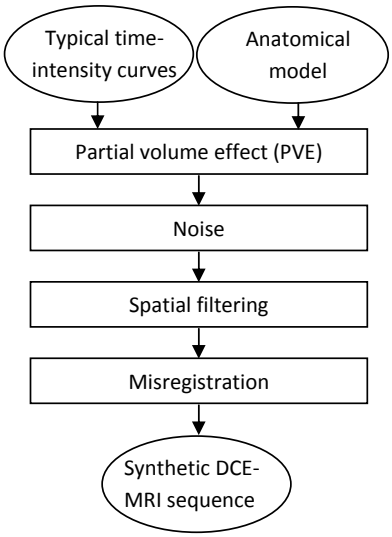

FIG. 5 – Flow chart for sequence synthesis

3.1.2 Dominant functional compartment

For the proposed model, four typical time-intensity curves are used. It is possible to compute some distance between each of them and the curve of a given voxel. The minimal distance indicates the dominant functional compartment. The underlying hypothesis for hard time-intensity based clustering is that dominant anatomical and functional compartment are the same : even for real data with no ground truth, reference segmentation used for validation can rather be considered as an anatomical one. However this is not true for all the voxels. For the proposed model, using Euclidean distance between curves, the dominant functional compartment is not the anatomical one for only 6 voxels out of 1264, i.e. less than 0.5%. Nevertheless noise, spatial filtering and misregistration may actually increase this difference.

3.2 Acquisition noise

Noise in MRI magnitude images is signal-dependent and commonly modelled by the Rician distribution [9]. Each frame is transformed in a noisy image with the Rician noise generator proposed in [10] that allows easy noise level adjustment. Examples are presented in figure 6c and d.

3.3 Spatial filtering

Reconstruction process is not exactly known and depends on the scanner. The real data we want to treat afterwards are acquired on a 1.5 T MR-scanner (General Electric Healthcare) with an ultra-fast gradient echo LAVA sequence with T_1 weighting with the following acquisition parameters : 15° flip angle, TR/TE 2.3 ms/1.1 ms. Interval between acquisitions is approximately 1.5 to 2 sec for the first 5 min and 9 sec for the last 6 min. The initial matrix size is 256×256 with pixel size between 1.172 mm and 1.875 mm for a 10 mm slice thickness. Each kidney can be included in a rectangular area which size varies between 47×35 and 84×59. It can be observed on their Fourier transform that images are filtered with a 2D spatial low-pass filter (approximate pass-band normalized frequencies : $0 - 0.5\pi$ rad\sample). Such a filter is thus applied to our data. For examples in figure 7b and d, dominant anatomical and functional compartments are different for about 5% of renal voxels.

3.4 Misregistration

As examination duration is about 10 minutes, kidney is moving essentially because of respiratory motion of the patient. A registration step can correct most of these movements. Nevertheless it can be noticed that some subpixel motions remain frequently, as reported in [11, 12, 13]. Imperfect registration has thus to be taken into account. For the sake of simplicity, no rotation nor elastic deformation is considered here. Every frame of the sequence is transformed with random independent horizontal and vertical translations drawn from a normal distribution with mean 0 and standard deviation 0.5 pixel. Required interpolation is performed with cubic splines. For the proposed example voxels with different dominant anatomical and functional compartment represent 8% of renal voxels.

3.5 Results

Examples of synthetic images are presented in figure 7 and can be compared with real frames of the kidney that our model is inspired from. Let us stress that our objective is not to reproduce exactly these frames.

4. CRITICAL ANALYSIS

The proposed model provides fairly realistic synthetic images of renal DCE-MRI with contrast agent injection despite rough modelling of some steps, in particular spatial filtering. The anatomical structure is simpler than the real one too. It can be noticed that the dark area around boundary between medulla and cavities in real image in figure 7b does not appear on synthetic image 7d, since typical contrast curves do not include such a temporal evolution. This model does not pretend to be universal nor to represent all the variety of kidney shapes and of average time-intensity curves depending on acquisition conditions. It does not allow to test

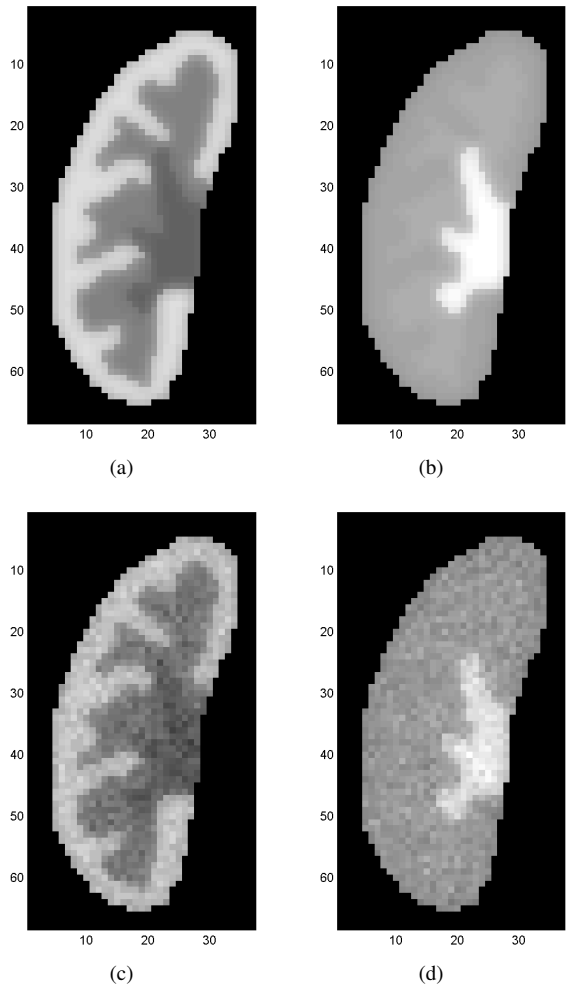

FIG. 6 – Example of synthetic images with partial volume effect but without noise during cortical peak (a) and late perfusion phase (b) ; the corresponding noisy images are (c) and (d)

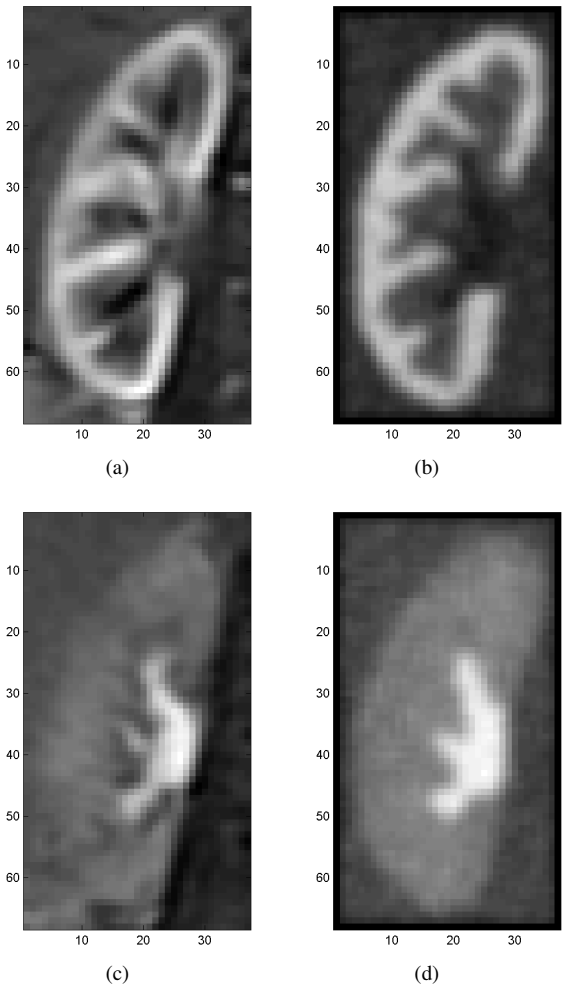

FIG. 7 – Example of real (a and c) and synthetic images (b and d) near cortical peak and in late perfusion phase

automatic extraction ok kidney since other organs are only modelled with a time-varying uniform background. It would be anyway relatively difficult to simulate their residual non-rigid motion after kidney registration.

However the model is simple to built and to use and does not require any simulation of the whole reconstruction process. Dominant anatomical and functional compartments can be distinguished and the origine of segmentation errors differentiated. For instance a method based on time-intensity curve clustering may correctly regroup voxels according to their dominant functional compartment but fail to recover anatomical segmentation.

The model highlights the difficulty to delineate compartment boundaries on blurred images and allows estimation of intra- and inter-operator variability for manual segmentation, which can then be compared with the one of semiautomatic methods. For instance, as a preliminary test, a manual segmentation of cortex, medulla and cavities was performed by two experts on the same synthetic sequence. The results were then compared with the anatomical ground truth provided by our model. Only about 90 % of pixels belonged to the same compartments in both any manual and ground truth segmentations, and a 15 % error rate was achieved for comparisons between the two manual segmentations.

We have adapted the model to pathological kidney simulation too by modifying typical time-intensity curve of cavities (with low contrast during the whole perfusion) and by choosing an anatomical model with dilated cavities and thinner parenchyma.

5. CONCLUSION

We proposed a method to generate synthetic DCE-MRI sequences of renal perfusion for objective assessment of methods based on analysis of voxel time-intensity curves. Our objective was to build sufficiently realistic images without simulation of the whole reconstruction process while making easy tuning of some parameters (noise level, spatial mixing of compartments for PVE simulation, registration error). We suggest to use such a model for a first validation of segmentation algorithms before assessment on real data in order to identify different types of error and to quantify their relative significance in global results.

The described model is two-dimensional but can easily be extended to a three-dimensional one from a volumetric hard segmentation by using 3D filters for anatomical model creation and for PVE simulation and by allowing out of plane translation for uncorrected residual motions. The typical time-intensity curves could also be generated thanks to some renal model with known parameters [14]. These parameters can then be estimated from the synthetic sequence and the estimated value could be compared with the true one.

Concerning independent component analysis applied to voxel time-intensity curves [4] or, more generally, methods resulting in segmentation with fractional labels, it can be difficult to decide meaning of these coefficients. The proposed model could help to interpret them and to decide if they are related or not to the $\alpha_j^{(i)}$.

REFERENCES

[1] Y. Sun, J.M.F. Moura, and H. Chien, "Subpixel registration in renal perfusion MR image sequence," in *Proceedings of the IEEE International Symposium on Biomedical Imaging : Macro to Nano (ISBI 2004)*, Arlington, VA, USA, 2004, vol. 1, pp. 700–3.

[2] T. Song, V.S. Lee, H. Rusinek, J.B. Sajous, and A.F. Laine, "Registration and segmentation of dynamic three-dimensional MR renography based on Fourier representations and k-means clustering," in *Proceedings of the 13th Scientific Meeting of the International Society for Magnetic Resonance in Medicine (ISMRM 2005)*, Miami, Florida, USA, 2005, 1 page.

[3] Y. Boykov and G. Funka-Lea, "Graph cuts and efficient N-D image segmentation," *International Journal of Computer Vision*, vol. 70, no. 2, pp. 109–131, 2006.

[4] F.G. Zoellner, M. Kocinski, A. Lundervold, and J. Roervik, *Bildverarbeitung fr die Medizin 2007*, chapter Assessment of Renal Function from 3D Dynamic Contrast Enhanced MR images Using Independent Component Analysis, pp. 237–241, Informatik aktuell. Springer Berlin Heidelberg, 2007.

[5] B. Chevaillier, Y. Ponvianne, J.L. Collette, D. Mandry, M. Claudon, and O. Pietquin, "Functional semi-automated segmentation of renal DCE-MRI sequences," in *Proceedings of the 33rd IEEE International Conference on Acoustics, Speech and Signal Processing (ICASSP 2008)*, Las Vegas (NV, USA), 2008, 525-528.

[6] B. Chevaillier, Y. Ponvianne, J.L. Collette, D. Mandry, M. Claudon, and O. Pietquin, "Functional semi-automated segmentation of renal DCE-MRI sequences using a growing neural gas algorithm," in *Proceedings of the 16th European Signal Processing Conference (EUSIPCO 2008)*, Lausanne (Switzerland), 2008, Electronic Proceedings, 4 pages.

[7] F. G. Zoellner, R. Sance, P. Rogelj, M.J. Ledesma-Carbayo, J. Roervik, A. Santos, and A. Lundervold, "Assessment of 3D DCE-MRI of the kidneys using non-rigid image registration and segmentation of voxel time courses," *Computerized Medical Imaging and Graphics*, vol. 33, pp. 171–181, 2009.

[8] M.A.G. Ballester, A. Zisserman, and M. Brady, "Estimation of the partial volume effect in MRI," *Medical Image Analysis*, vol. 6, pp. 389–405, 2002.

[9] R.D. Nowak, "Wavelet-based Rician noise removal for magnetic resonance imaging," *IEEE Transactions on Image Processing*, vol. 8, no. 10, pp. 1408–19, 1999.

[10] G. Ridgway, "Rice/rician distribution, http ://www.mathworks.com/matlabcentral/fileexchange," 2007.

[11] Y. Sun, M.-P. Jolly, and J.M.R. Moura, "Integrated registration of dynamic renal perfusion MR images," in *Proceedings of the International Conference on Image Processing (ICIP 2004)*, Singapore, 2004, vol. Vol. 3, pp. 1923–6.

[12] T. Song, V.S. Lee, H. Rusinek, M. Kaur, and A.F. Laine, "Automatic 4-D registration in dynamic MR renography based on over-complete dyadic wavelet and Fourier transforms," in *Proceedings of the 8th Conference on Medical Image Computing and Computer-Assisted Intervention (MICCAI 2005)*, Palm Springs CA, USA, 2005, pp. 205–13.

[13] T. Song, V.S. Lee, H. Rusinek, S. Wong, and A.F. Laine, "Four dimensional MR image analysis of dynamic renography," in *Proceedings of the 28th Annual International Conference of the IEEE Engineering in Medicine and Biology Society (EMBS 2006)*, Piscataway, NJ, USA, 2006, pp. 3134–3137.

[14] S.P. Sourbron, H.J. Michaely, M.F. Reiser, and S.O. Schoenberg, "MRI-measurement of perfusion and glomerular filtration in the human kidney with a separable compartment model," *Investigative Radiology*, vol. 43, no. 1, pp. 40–48, 2008.